CHAPTER - 4

RESULT AND DISCUSSION

4. 1: HIGH T_C CUPRATES SUPERCONDUCTORS

Table 4.1: Variation of superconducting order parameter (Δ) with temperature for various magnetic order parameter (ϕ).

Temperature (k)	Δ (eV) for ϕ = 0.0001 eV	Δ (eV) for ϕ = 0.001 eV	Δ (eV) for ϕ = 0.005 eV
1.00	0.005414	0.004514	0.000514
5.00	0.005414	0.004514	0.000514
10.00	0.005404	0.004504	0.000504
15.00	0.005311	0.004411	0.000411
20.00	0.005033	0.004133	0.000133
21.50	0.004900	0.004000	0.000000
25.00	0.004475	0.003575	0.000000
30.00	0.003464	0.002564	0.000000
35.00	0.001119	0.000219	0.000000
35.19	0.000900	0.000000	0.000000
35.58	0.000000	0.000000	0.000000

Table 4.2: Variation of superconducting order parameter (Δ) with magnetic order parameter (ϕ) at different temperature (T).

Magnetic order parameter ϕ (eV)	Δ (eV) for T = 20 k	Δ (eV) for T = 25 k	Δ (eV) for T = 30 k	Δ (eV) for T = 32.5 k	Δ (eV) for T = 35 k
0.00000	0.005133	0.004575	0.003564	0.002734	0.001219
0.00001	0.005123	0.004565	0.003554	0.002724	0.001209
0.00005	0.005083	0.004525	0.003514	0.002684	0.001169
0.00010	0.005033	0.004475	0.003464	0.002634	0.001119
0.00050	0.004633	0.004075	0.003064	0.002234	0.000719
0.00100	0.004133	0.003575	0.002564	0.001734	0.000219
0.00500	0.000133	0.000000	0.000000	0.000000	0.000000

Table 4.3: Variation of magnetic order parameter (ϕ) with transition temperature (T_C)

Transition temperature T_C (k)	**Magnetic order parameter ϕ (eV)**
5	0.00551
10	0.00556
15	0.00575
20	0.00600
25	0.00619
30	0.00628
35	0.00622
40	0.00597
45	0.00535
46	0.00514
47	0.00487
48	0.00000

Table 4.4: Variation of transition temperature (T_C) with spin exchange coupling between localized electrons (J).

Exchange interaction between localized electrons J (meV)	**Transition temperature T_C (k)**
1	7.75
5	13.81
10	17.54
15	20.14
20	22.21
25	23.95
30	25.47
35	26.82
40	28.05

Table 4.5: Variation of transition temperature (T_C) with spin exchange coupling between localized and conduction electrons (τ).

Exchange interaction between localized and conduction electrons τ(meV)	Transition temperature T_C (k)
1	46.02
2	36.51
3	31.86
4	28.92
5	26.82
6	25.22
7	23.95
8	22.88
9	21.99
10	21.22

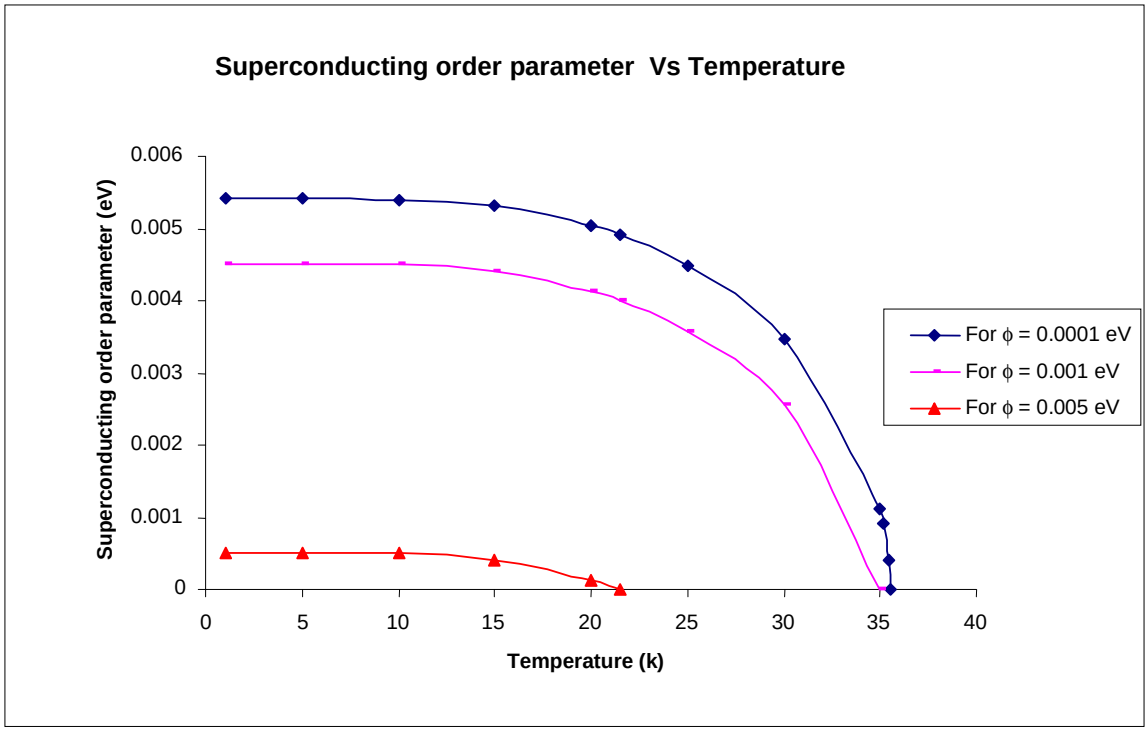

Fig. 4.1: Variation of superconducting order parameter (Δ) with temperature (T).

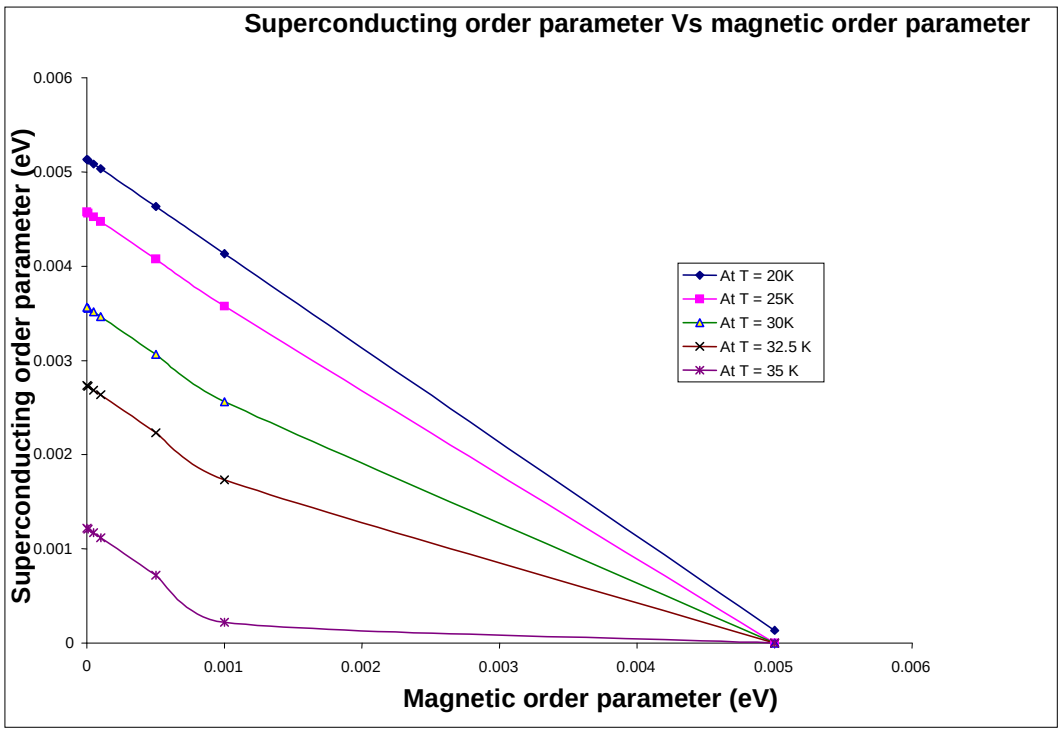

Fig. 4.2: Variation of superconducting order parameter (Δ) with magnetic order parameter (ϕ).

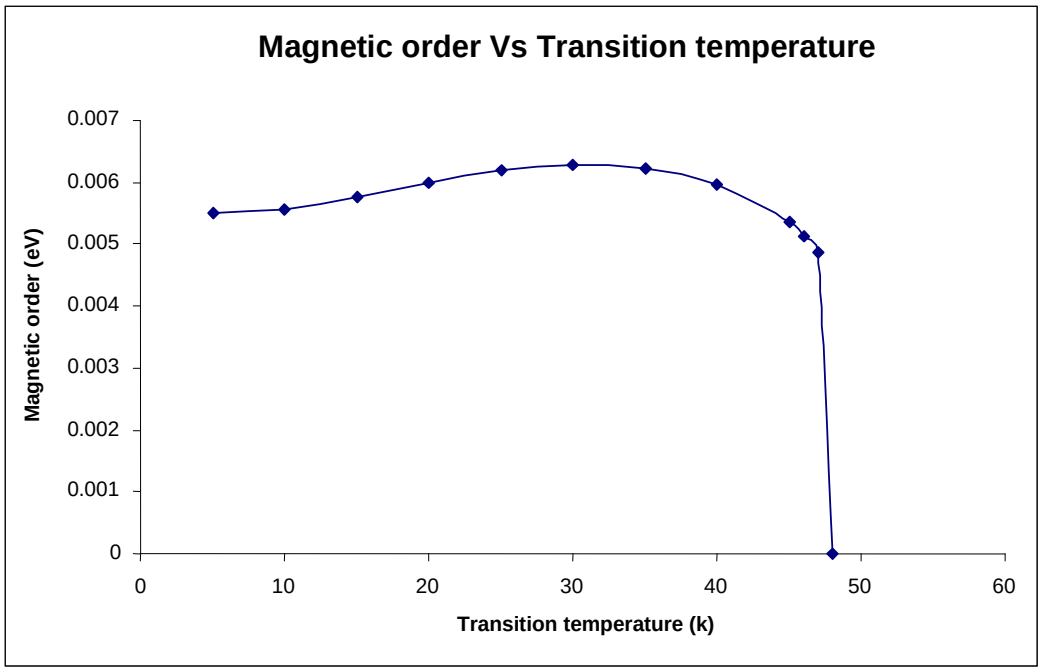

Fig. 4.3: Variation of magnetic order parameter (ϕ) with transition temperature (T_C).

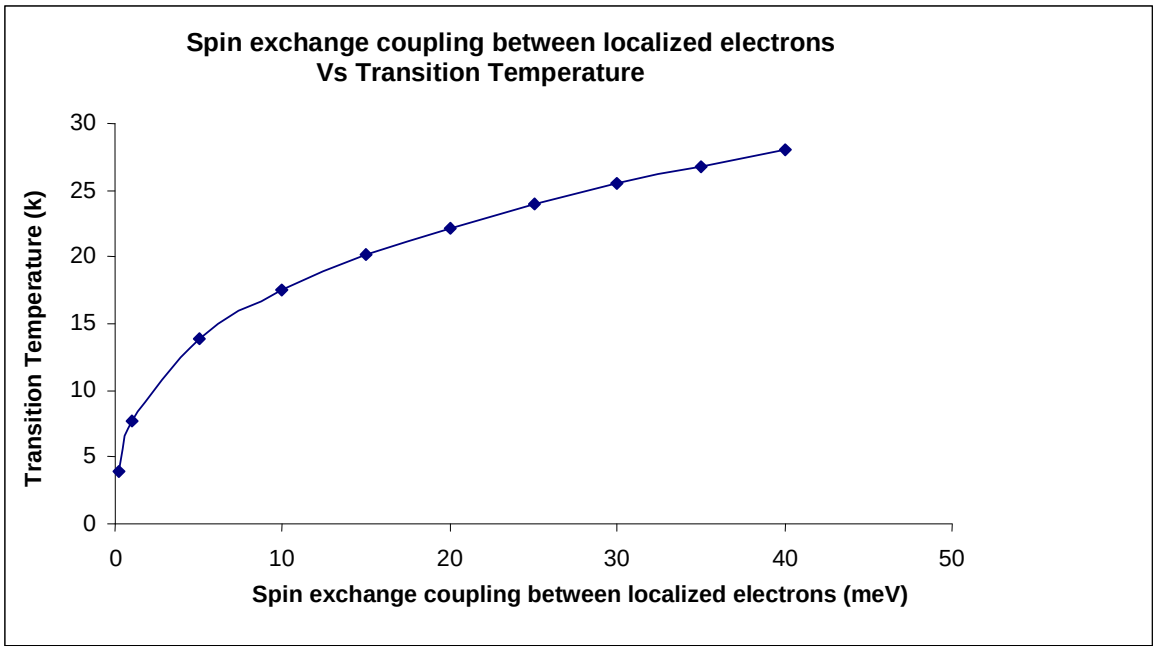

Fig. 4.4: Variation of transition temperature (T_C) with spin exchange coupling between localized electrons (J).

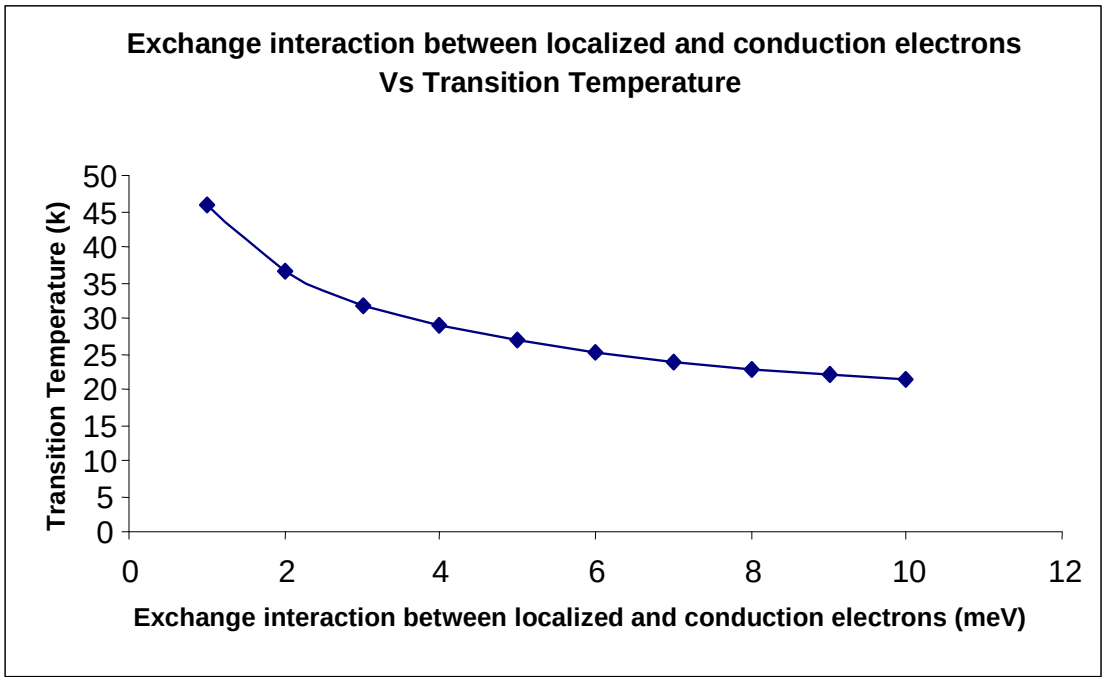

Fig. 4.5: Variation of transition temperature (T_C) with exchange interaction between localized and conduction electrons (τ).

In this session the effect of magnetic order on superconducting order parameter and transition temperature in high T_C cuprates has been studied. The double time retarded Green's function technique has been used in the spirit of mean field approximation in order to obtain the expression for superconducting order parameter *(Δ).* The expression is found to be depending on the magnetic order parameter and temperature. The numerical analysis shows the destructive effect of magnetic order on superconducting order parameter which is qualitatively similar to that of transition temperature.

Figure (4.1) is plotted between superconducting order parameter *(Δ)* and temperature *(T)* for various magnetic order parameter (ϕ). The above curve in the figure (4.1) represent the variation of Δ with respect to T for ϕ = 0.0001 eV and the lower one represent the variation ofΔ with respect to T for ϕ = 0.001 eV**.** From the curve it is clear that as temperature increases, the superconducting order parameter monotonically

decreases and become zero at transition temperature T_C. The another important feature of the curve is that at low magnetic order, superconducting order parameter as well as transition temperature reached at the larger value and their values decrease as increase the magnetic order.

Figure (4.2) is plotted between superconducting order parameter and magnetic order parameter for different temperatures. Figure shows that for temperature 20 k, 25 k and 30 k superconducting order parameter decreases linearly with increasing magnetic order parameter. But at the temperature 32.5 k and 35 k, which is near to transition temperature (37 k), this linearity is violated and superconducting order first suddenly and then after rate of decrease slow down with increase of magnetic order. It looks reasonable that at close to transition temperature, more fluctuation produce, which reduce the stability of superconducting material and a small increase in magnetic order can much reduce the superconducting order. This also shows from the figure (4.2) that at close to transition temperature the area of co-existence of magnetism and superconductivity also decreases.

Figure (4.3) shows the variation of transition temperature (T_C) with magnetic order parameter (ϕ). Figure shows that magnetic order parameter (ϕ) increases with T_C when T_C is below than 35 k and when T_C cross the 35 k, magnetic order start to decrease. It looks reasonable that at high temperature, single particle tunneling dominant the cooper pair tunneling due to breaking of cooper pairs and as observed by P. Ahalawat et. al. (2007) for single particle tunneling, magnetic order much suppresses the superconducting order parameter, T_C decrease.

This shows that magnetic order can support superconductivity when T_C is below 35 k. Therefore for those compounds where T_C is upto 35 k, this present Hamiltonian (equation 3.5) is the possible model for them. Further for cuprates having T_C below which 35 k, magnetic order will co-exist with superconductivity and could be helpful as ϕ increases with T_C as shown in the figure.

To analyze the role of spin exchange coupling (J) between localized electrons in the superconducting state, figure (4.4) is plotted, which shows that with increase in spin exchange coupling (J), T_C first sharply increase & then for higher values of J, this rate of increase of T_C slows down with J. So this spin exchange interaction between localized sites, plays an important role in formation of cooper pairs which overcomes the repulsive coulomb potential between the electrons and hence helps to increase the transition temperature T_C.

From the curve it is also clear that at $J = 0$, transition temperature T_C is 5 k, this shows that in absence of spin exchange coupling between localized electrons, there is some residual cooper pairs which gives its superconducting state at very low transition temperature. This will be due to phononic contribution and some other interactions (interlayer interaction) which help to make cooper pairs. So, this spin exchange interaction is not necessary to obtain superconducting state but very important to stabilize superconducting order and help to increase transition temperature (T_C).

Figure (4.5) shows the variation of transition temperature (T_C) with exchange interaction between localized and conduction electrons (τ). Figure shows that as increase the exchange interaction between localized and conduction electrons, transition temperature (T_C) decreases. At close to transition temperature this exchange interaction between localized and conduction electrons (τ) dominant the spin exchange coupling between localized electrons (J) and hence this reduce the transition temperature (T_C).

4. 2: IRON PNICTIDE SUPERCONDUCTORS (OXYPNICTIDES)

Table 4.6: Variation of magnetization ($\bar{S}$) with temperature for LaFeAsO with $J_\perp$ = 0 meV and $J_\perp$ = 3 meV.

Temperature (k)	Magnetization $\bar{S}$ with $J_\perp$ = 3 meV
0	0.1896
10	0.1896
20	0.1896
30	0.1896
40	0.1895
50	0.1893
60	0.1887
70	0.1873
80	0.1847
90	0.1810
100	0.1753
110	0.1675
120	0.1569
130	0.1417
140	0.1180
141	0.0000

Table 4.7: Variation of magnetization ($\bar{S}$) with temperature for LaFeAsO with $J_\perp$ = 0 meV and $J_\perp$ = 3 meV.

***T*emperature (k)**	**Magnetization $\bar{S}$ with $J_\perp$ = 0 meV**	**Magnetization $\bar{S}$ with $J_\perp$ = 3 meV**
0	0.1883	0.1896
10	0.1883	0.1896
20	0.1883	0.1896
30	0.1883	0.1896
40	0.1882	0.1895
50	0.1876	0.1893
60	0.1861	0.1887
70	0.1833	0.1873
80	0.1785	0.1847
90	0.1713	0.1810
100	0.1608	0.1753
110	0.1454	0.1675
120	0.1210	0.1569
130	0.0000	0.1417
140	0.0000	0.1180
141	0.0000	0.0000

Table 4.8: Variation of magnetization ($\bar{S}$) with temperature for PrFeAsO with $J_\perp$ = 0 meV and $J_\perp$ = 3 meV.

***T*emperature (k)**	**Magnetization $\bar{S}$ with $J_\perp$ = 0 meV**	**Magnetization $\bar{S}$ with $J_\perp$ = 3 meV**
0	0.1830	0.1841
10	0.1830	0.1841
20	0.1830	0.1841
30	0.1830	0.1841
40	0.1827	0.1840
50	0.1816	0.1836
60	0.1790	0.1826
70	0.1746	0.1804
80	0.1672	0.1770
90	0.1560	0.1715
100	0.1390	0.1638
110	0.1100	0.1528
120	0.0000	0.1370
130	0.0000	0.1110
131	0.0000	0.0000

Table 4.9: Variation of magnetization ($\bar{S}$) with temperature for CeFeAsO with $J_\perp$ = 0 meV and $J_\perp$ = 3 meV.

***T*emperature (k)**	**Magnetization $\bar{S}$ with $J_\perp$ = 0 meV**	**Magnetization $\bar{S}$ with $J_\perp$ = 3 meV**
0	0.1870	0.1880
10	0.1870	0.1880
20	0.1870	0.1880
30	0.1870	0.1880
40	0.1869	0.1878
50	0.1865	0.1872
60	0.1852	0.1860
70	0.1828	0.1838
80	0.1786	0.1804
90	0.1725	0.1754
100	0.1634	0.1685
110	0.1506	0.1590
120	0.1312	0.1470
130	0.0000	0.1284
140	0.0000	0.1124
143	0.0000	0.0000

Table 4.10: Néel temperature (T_N) with and without out-of-plane coupling ($J_\perp$)

Compound	**T_N (k) Experiment**	**T_N (k) With $J_\perp$ = 0 meV**	**T_N (k) with $J_\perp$ = 3 meV**
LaOFeAs	137	120	140.58
CeOFeAs	148	123.16	143.51
PrOFeAs	127	109.33	129.27

Table 4.11: Variation of Néel temperature (T_N) with out-of-plane coupling between Fe-As ($J_\perp$) for LaFeAsO.

$J_\perp$ (meV)	T_N (k)
0	120.00
1	126.95
2	133.80
3	140.58
4	147.30
5	153.97
6	160.60

Table 4.12: Variation of Néel temperature (T_N) with out-of-plane coupling between Fe-As ($J_\perp$) for PrFeAsO and CeFeAsO.

$J_\perp$ (meV)	T_N (k) for PrFeAsO	T_N (k) for CeFeAsO
0	109.33	123.16
1	116.06	130.02
2	122.70	136.80
3	129.27	143.51
4	135.79	150.17
5	142.25	156.77
6	148.67	163.33

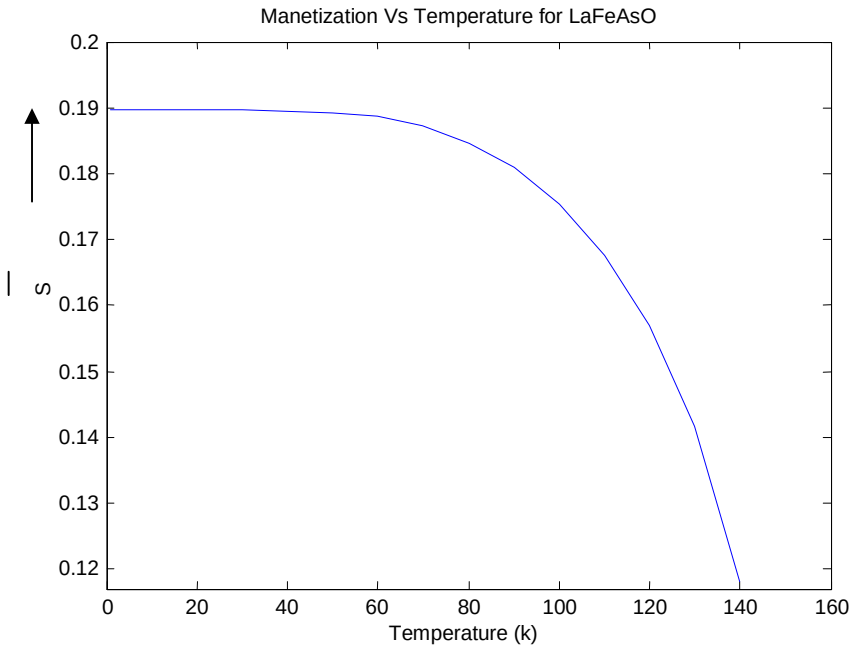

Fig. 4.6: Curve showing variation of magnetization ($\bar{S}$) with temperature (k) for LaFeAsO

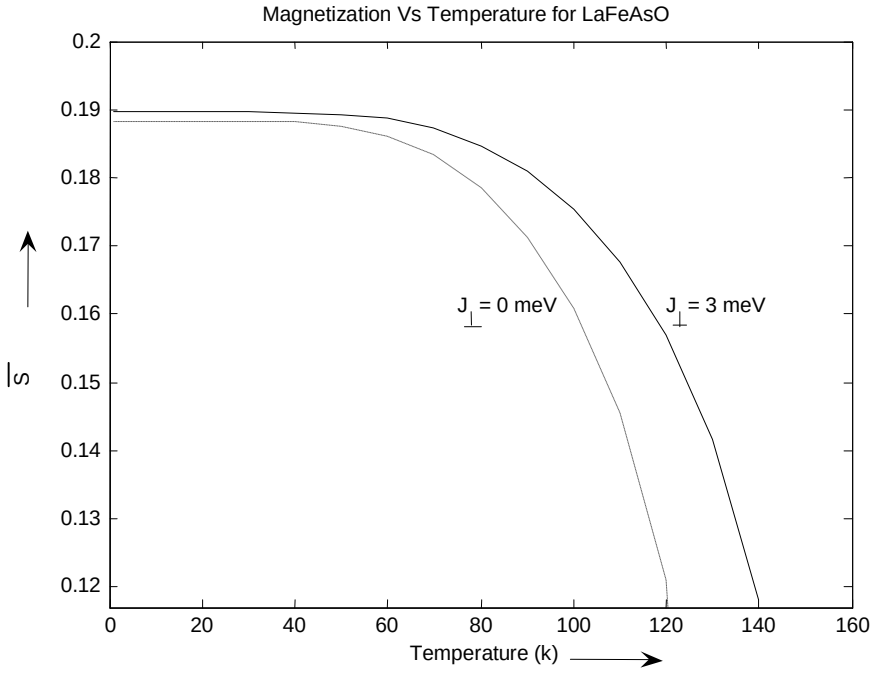

Fig. 4.7: Curve showing variation of magnetization ($\bar{S}$) with temperature (k) for LaFeAsO with $J_{\perp} = 0$ meV and $J_{\perp} = 3$ meV.

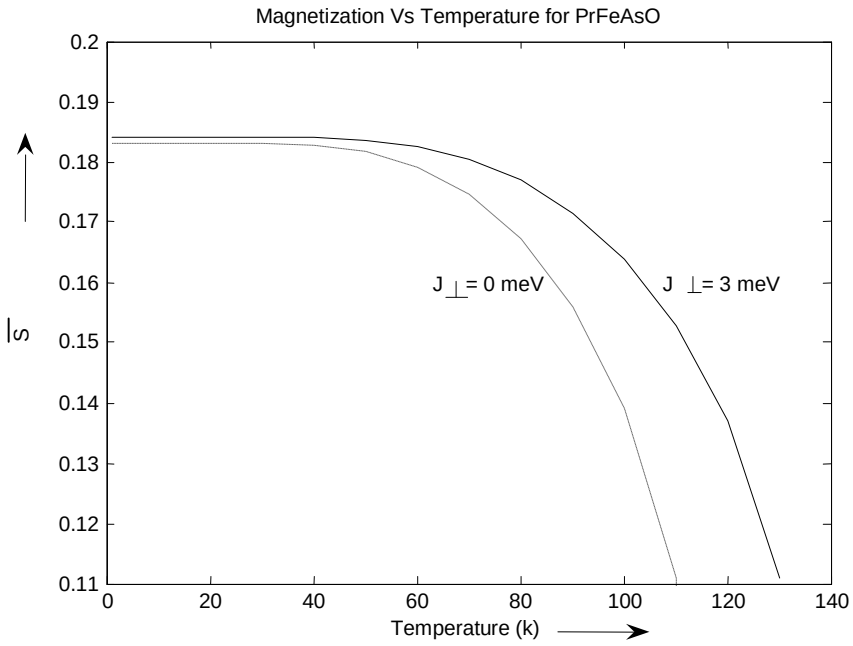

Fig. 4.8: Curve showing variation of magnetization ($\bar{S}$) with temperature (k) for PrFeAsO with $J_{\perp} = 0$ meV and $J_{\perp} = 3$ meV.

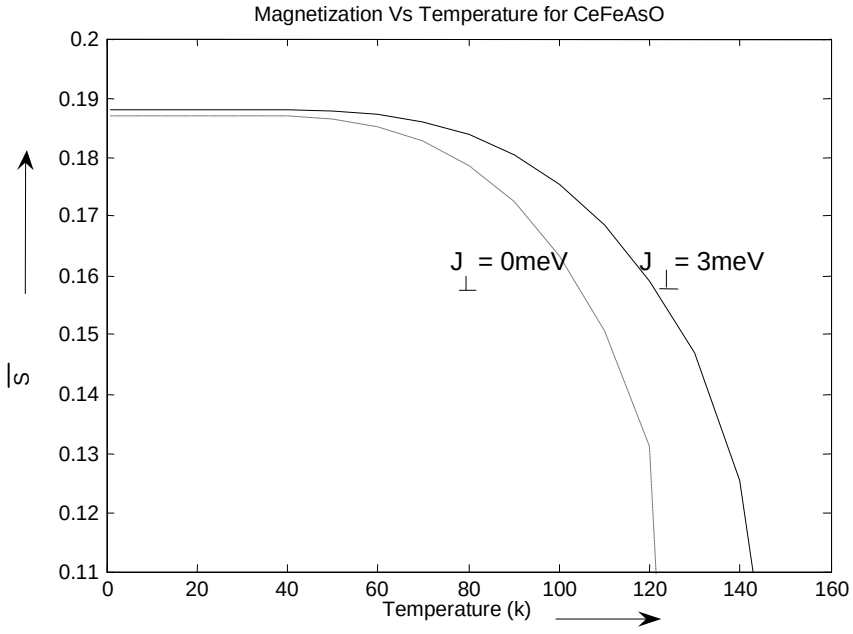

Fig. 4.9: Curve showing variation of magnetization ($\bar{S}$) with temperature (k) for CeFeAsO with $J_{\perp} = 0$ meV and $J_{\perp} = 3$ meV.

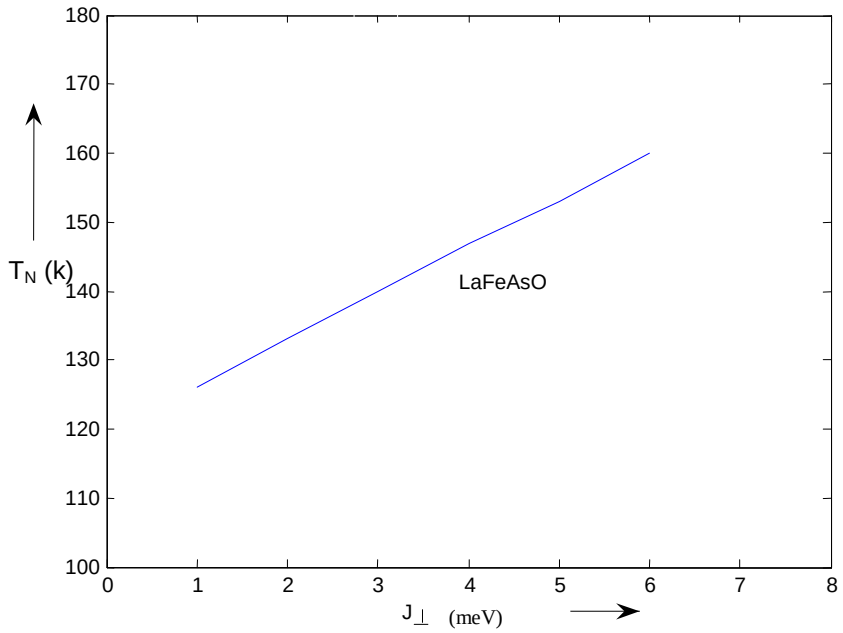

Fig. 4.10: Curve showing variation of Néel temperature (T_N) with out-of-plane coupling between Fe-As ($J_\perp$) for LaFeAsO.

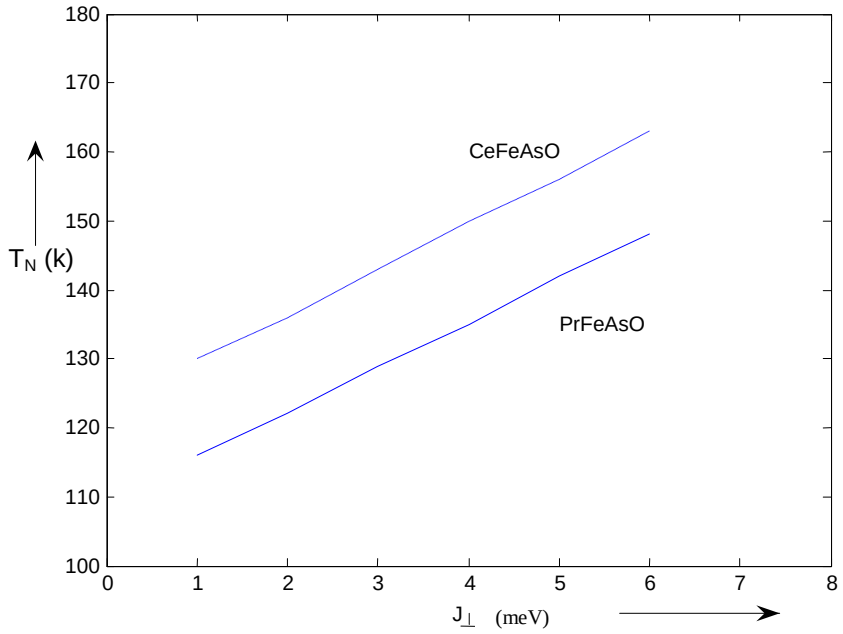

Fig. 4.11: Curve showing variation of Néel temperature (T_N) with out-of-plane coupling between Fe-As ($J_\perp$) for PrFeAsO and CeFeAsO.

In this section, the numerical results obtained for sublattice magnetization and Néel temperature has been presented for '1111' iron pnictides from eq. (3.66) and eq. (3.67) respectively. In the present model of pnictides, the stripes of Fe spins with three in plane exchange couplings and one out-of-plane Fe-As exchange coupling (above and below Fe plane) has been considered. As suggested by J. Zhao and T. Yildrim that in pnictides nearest, next nearest and second next nearest neighbour interactions are appreciable, nearest antiferromagnetic coupling (J_1), nearest neighbour ferromagnetic coupling (same stripe, J_2) and next nearest neighbour antiferromagnetic coupling (J_3) has considered. In addition to this the out-of-plane Fe-As exchange interaction ($J_\perp$) has also considered after the report of Fe-As interaction in iron pnictides.

Using eq. (3.66), self consistently $\bar{S}$ is calculated with temperature. During the numerical calculation these interactions are estimated as J_1 = 30 meV, J_2 = 7 meV, J_3 = 17 meV & $J_\perp$ = 3 meV for LaOFeAs J_1 = 31 meV, J_2 = 7 meV, J_3 = 18 meV, $J_\perp$ = 3 meV for CeOFeAs and J_1 = 27 meV, J_2 = 7 meV, J_3 = 16 meV, $J_\perp$ = 3 meV for PrOFeAs (as per the condition $J_3 > J_1/2$). The plot for LaOFeAs is shown in Fig. 4.6. It is clear from the curve that the magnetization decreases as the temperature increases and becomes zero at temperature $\geq T_N$.

In order to examine the effect of $J_\perp$ on magnetization, sublattice magnetization ($\bar{S}$) with temperature is plotted for $J_\perp$ = 0 meV and 3 meV in Fig. 4.7 (keeping the in-plane exchange couplings constant). It is evident from the curve that as $J_\perp$ increases the sublattice magnetization also increases at all temperature $\leq T_N$. It is also seen from the curve that increase in $J_\perp$, increases T_N as well.

This implies from these curves that $J_\perp$ increases T_N, helping to maintain the long range order and thus has an important role in magnetic dynamics of '1111' pnictides. It is imperative here to focus on the fact that all 122 pnictides has T_N greater than '1111' pnictides. As all 122 compounds have two FeAs layers per unit cell and interaction

between the two layers exist, it argue that this additional channel leads to further enhancement of T_N.

Néel temperature of PrOFeAs and CeOFeAs based on this model with out-of-plane and without out-of-plane interactions has also calculated from equation (3.67). The plots are shown in Fig. 4.8 & Fig. 4.9 respectively and the results are listed in Table 4.10.

It is clear from the table 4.10 that for $J_\perp$ = 3 meV, theoretical value of Néel temperature is close to the experimental values and hence our assumption of $J_\perp$ is justified. Results also indicate that only in plane exchange interactions as suggested by Yildrim et al. are not sufficient to get the Néel temperature of the pnictides. This result finds relevance in view of the work done by Yildrim et al., where they concluded that Fe moment is always present in these materials and even a small amount of moment on Fe reduces the As-As interaction and increases the Fe-As interaction. These results of Néel temperature based on anisotropic Heisenberg model with out-of- plane interaction further strengthen the presence of Fe-As interactions in these materials. Earlier role of Fe-As interaction was studied for the structural transformation but the present result show that it has role to play in magnetic properties of the pnictides as well.

Another important result is obtained from plot of Néel temperature with $J_\perp$ from equation (3.67) for LaOFeAs. The plot is shown in Fig. 4.10. It is clear from the curve that T_N increases linearly with $J_\perp$. Similar result also found from the plot of Néel temperature with $J_\perp$ for PrFeAsO and CeFeAsO, shown in Fig. (4.11). From this result along with result from Fig. 4.7, it can conclude that $J_\perp$ helps in increasing the Néel temperature and maintaining the long range order in ‘1111’pnictides.